

# 1 ***In silico* dynamic characterization of the femur: physiological versus** 2 **mechanical boundary conditions**

3 **E. Reina-Romo, J. Rodríguez-Vallés, J.A. Sanz-Herrera**

4 *School of Engineering, University of Seville, 41092 Seville (Spain)*

5

## 6 **Abstract**

7 It is established that bone tissue adapts and responds to mechanical loading. Several  
8 studies have suggested an existence of positive influence of vibration on the bone  
9 mass maintenance. Thus, some bone regeneration therapies are based on vibration of  
10 bone tissue under circumstances of disease to stimulate its formation. Frequency of  
11 loading should be properly selected and therefore a correct characterization of the  
12 dynamic properties of this tissue may be critical for the success of such orthopedic  
13 techniques. On the other hand, many studies implement vibration techniques with *in*  
14 *silico* models. Numerical results are exclusively dependent on properties of bone  
15 tissue, i.e. geometry, density distribution and stiffness, as well as boundary conditions.  
16 In the present study, the influence of boundary conditions and material properties on  
17 the dynamic characteristics of bone tissue was explored in a human femur. Bone shape  
18 and density were directly reconstructed from computer tomographies, whereas  
19 natural frequencies and modes of vibration were obtained for different boundary  
20 conditions including physiological and mechanical ones. Results of this study show the  
21 moderate effect of material properties compared to the much substantial effect of  
22 boundary conditions. A factor of 2 in the natural frequency was obtained depending on  
23 imposed boundary conditions, highlighting the importance in the selection of  
24 appropriate conditions in the analysis of the bone organ.

25 **Keywords:** Bone Mechanics, Finite Element Method, Natural Frequency, Modal  
26 Analysis.

27

## 28 **1. Introduction**

29 It is established that bone tissue adapts and responds to mechanical loading. The  
30 characteristics of the mechanical loads, such as peak magnitude of ground reaction  
31 force, peak rate of force production, and repetition rate of these loads, are known to  
32 be important in regulating bone regeneration [1]. According to experimental studies,  
33 maximum bone formation directly depends on loading frequencies and targeted  
34 locations of bones [2-6]. Zhao et al. [7] have demonstrated in an *in vivo* study  
35 performed on mice that the application of loads with frequencies near the natural  
36 frequency of bone favors bone formation. Rubin et al. [8] have shown that very-low-

37 magnitude, frequency vibration of 30Hz, increases significantly (by 34.2 %) the density  
38 of the trabecular bone in the proximal human femur compared to controls. Therefore,  
39 a possible application to increase bone mass under circumstances of disease would be  
40 to apply vibration loading stimulation: whole-body vibration, bone bending, axial  
41 loading, and joint loading [10-13]. Whole-body vibration seems to prevent/reverse  
42 sarcopenia and possibly osteoporosis [9]. Vibration analysis techniques have been  
43 used successfully to determine mechanical properties of human bone [14], to monitor  
44 fractures [15-16], to quantify the stability of dental implants [17-18] and to detect  
45 forms of femoral prosthesis loosening [19]. In the orthopaedic field, this technique  
46 may have potential due to apparent benefits it offers.

47 The vibration characteristics of bone have been analyzed both experimentally [10,20-  
48 21] and numerically [7,14,19,22-23]. Although Weiss et al. [24] have shown the  
49 importance of the boundary conditions in vibration studies in a hip endoprosthesis  
50 system, the most commonly used boundary conditions are the free ones [14,22],  
51 which are known to be far from the *in vivo* environment. For example, Campoli et al.  
52 [22] already analyzed by means of finite element analysis how the natural frequencies  
53 changed by varying the density and shape of the human femur in free boundary  
54 conditions. The behavior of the femoral head prosthesis has also been analyzed *in*  
55 *silico* with modal analyses assuming free boundary conditions and constant mechanical  
56 properties [23]. Pérez & Seral-García [19] used other boundary conditions to simulate  
57 numerically the change in the resonance frequency during the osseointegration  
58 process of a cementless human hip system. In that study mechanical properties were  
59 assigned based on the level of Hounsfield Unit (HU).

60 A number of studies have already shown that geometry and material properties at  
61 boundaries and spatiotemporal distributions within bone have a profound effect on  
62 bone mechanobiology variables such as fluid velocities and pore pressures [25-26].  
63 However, as far as the authors know, there is no vibration study that has numerically  
64 analyzed the influence of the properties of bone tissue, i.e. geometry, density  
65 distribution and stiffness, as well as boundary conditions on the dynamic  
66 characteristics of bone. Therefore, the aim of this study is to analyze *in silico* the  
67 dynamic characteristics of a human femur under different boundary conditions and  
68 assumptions found in the literature. Different numerical set-ups of the femur, which  
69 differed in the material properties assignment and boundary conditions, have been  
70 analyzed. On the one hand, either constant material properties or a technique based  
71 on HU was used. On the other hand, four different boundary conditions are  
72 implemented and analyzed: free, diaphysis, condyle and physiological boundary  
73 conditions with the purpose of determining the dynamic characteristics of the femur  
74 as closely as possible as they can be found *in vivo*. Using the information provided in  
75 this study, a proper determination of bone resonance frequencies could be conducted,  
76 which in turn may be of special relevance to calibrate existing vibration therapies

77 performed clinically and to help to improve the treatment of some diseases such as  
78 the osteoporosis.

## 79 **2. Materials and Methods**

80

### 81 *2.1. Geometry*

82 A set of 664 computer axial tomographies (CATs) of a cadaveric adult male human  
83 femur were selected. CAT resolution includes a pixel size of 0.78x0.78 mm and a slice  
84 thickness of 0.8 mm. Geometry was built by means of the software MIMICS 10.0<sup>®</sup> as  
85 follows: outer (cortical) and inner (marrow) regions were selected manually at  
86 diaphyseal region attending to the grey scale level of pictures, as well as spongy bone  
87 at proximal areas. Other regions of non interest in the study, such as hip, knee or tibia  
88 were not included in the geometry. Then, 3D geometry of the right femur was  
89 reconstructed by using the above mentioned software.

### 90 *2.2 Boundary conditions*

91 Four different boundary conditions are implemented and analyzed in the paper,  
92 namely, free, diaphysis (fig. 1a), condyle (fig. 1b) and physiological boundary  
93 conditions (fig. 1c) [27]. They are explained next.

#### 94 *Free boundary conditions*

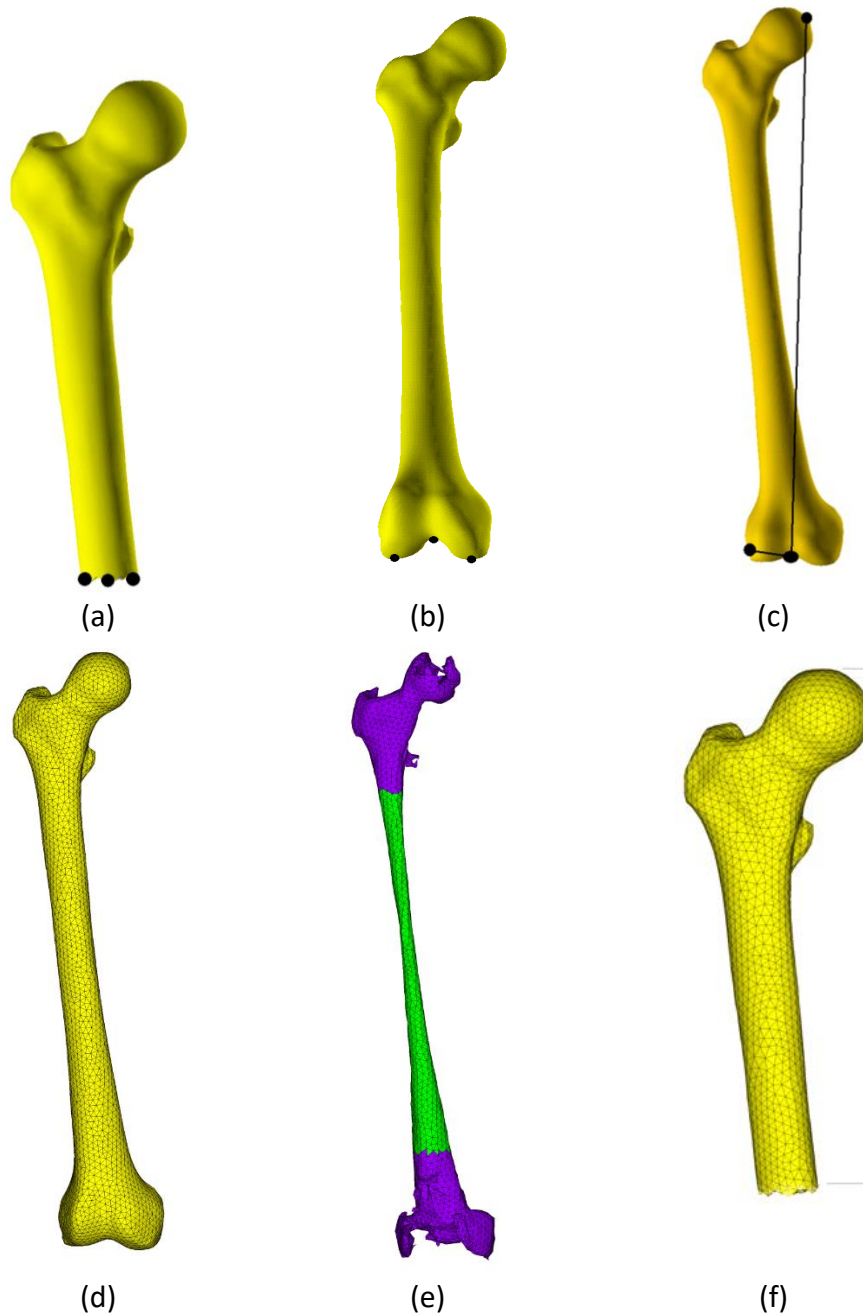
95 In this case, femur was free of loading and displacement restrictions. This is the most  
96 suitable boundary conditions used both in experimental modal analysis [14,20] as well  
97 as numerical modal analysis of the bone tissue [14,22-23], due to both reliability and  
98 simplicity at the laboratory level and finite element analysis.

#### 99 *Diaphysis boundary conditions*

100 Displacements are prescribed at nodes in the mid-diaphysis where the cut was  
101 performed (see fig. 1a) [27,28]. Both nodes at exterior (cortical) and interior (marrow)  
102 regions were considered.

#### 103 *Condyle boundary conditions*

104 All the displacements are prescribed at the three nodes shown in fig. 1b in the distal  
105 condyles.



106  
 107 **Figure 1.** Finite element model of different implemented boundary conditions: (a) diaphysis,  
 108 (b) condyle and (c) physiological. Tetrahedral finite element mesh at (d) the exterior (cortical),  
 109 (e) the interior (marrow and spongy bone) regions; (f) finite element mesh for the diaphysis  
 110 boundary conditions analysis.

111 *Physiological boundary conditions*

112 The so-called physiological conditions are the ones proposed by Speirs et al. [27]. In  
 113 that work, authors conclude that this set of boundary conditions is the one that best  
 114 represents the femur deformations at real conditions. They are implemented as  
 115 follows (fig. 1c). First, the three translational degrees of freedom at a node placed in  
 116 the knee centre are prescribed, specifically at the joint of the tibia with the femur.

117 Then, two displacements at a node in the femur head are also prescribed. At this node,  
118 only the displacement in the direction along an axis towards the knee center is  
119 allowed. Finally, the sixth degree of freedom was constrained at a node placed on the  
120 distal lateral epicondyle in order to avoid rigid body motions (see fig. 1c).

### 121 *2.3 Finite element mesh*

122 Femur geometry was exported into the finite element software ANSYS 14.5®.  
123 Tetrahedral 8 node 3D quadratic elements (SOLID 185) were used including 60227  
124 elements and 12020 nodes in the femur mesh (see figs. 1d and e).

125 For diaphysis boundary conditions, a different finite element model was used (see fig.  
126 1f). In this case a cut was performed at the mid-diaphysis [27] (see fig. 1f).

### 127 *2.4 Mechanical properties of bone tissue*

128 Linear, elastic and isotropic mechanical properties were considered in this study  
129 [14,22]. Material properties were characterized by Young's modulus and Poisson's  
130 ratio. Nonetheless, femur domain was considered to be heterogeneous, such that each  
131 finite element in the model was featured by different mechanical parameters.  
132 Mechanical properties have been assigned with two different approaches: depending  
133 on the level of HU, regardless its location and, manually, considering three different  
134 material sets.

135 Firstly, the technique based on HU was implemented. Bone density was linearly  
136 correlated with HU from 0,5 g/cm<sup>3</sup> of the spongy bone to 1,952 g/cm<sup>3</sup> of the cortical  
137 bone [22]. Mathematically, this relation attends to the following curve:

$$138 \quad \rho \text{ (g/cm}^3\text{)} = 0,000968 \times HU + 0,5 \quad (1)$$

139 where  $\rho$  is the bone tissue density and  $HU$  is the Hounsfield Unit, which varied from 0  
140 to 1500. Bone density is related to the mechanical properties following Beaupre et al.  
141 [29] as:

$$142 \quad \text{If } \rho \leq 1,2 \text{ g/cm}^3 \text{ ; } E = 2014\rho^{2,5} \text{ (MPa), } \nu = 0,2 \quad (2)$$

$$143 \quad \text{If } \rho > 1,2 \text{ g/cm}^3 \text{ ; } E = 1763\rho^{3,2} \text{ (MPa), } \nu = 0,32$$

144 where  $E$  and  $\nu$  are the Young's modulus and Poisson's ratio, respectively. A set of 10  
145 values of density, uniformly distributed from lower (0,5 g/cm<sup>3</sup>) to upper (1,952  
146 g/cm<sup>3</sup>) bounds, respectively, were considered. Consequently, a number of 10  
147 different pairs ( $E$ ,  $\nu$ ) were estimated for the mechanical properties along the bone  
148 tissue through Eq. (2) according to its estimated density. This was included as different  
149 materials in the finite element mesh by using utilities of MIMICS 10.0®  
150 and ANSYS ICEM 14.5® softwares.

151 Secondly, the finite element model was tested assuming constant mechanical  
152 properties. Three different material sets were distinguished: cortical bone, bone  
153 marrow and spongy bone (fig. 1e). In this case, mechanical properties are given in  
154 table 1.

Material	Density (kg/m <sup>3</sup> )	Young's modulus (GPa)	Poisson's ratio (-)
Cortical bone [22]	1800	13	0,3
Bone marrow [29]	1060	0,001	0.5
Spongy bone [22]	500	0,6	0,12

155

156 **Table 1.** Mechanical properties of finite element model of the femur when considered as  
157 constant.

### 158 *2.5 Analysis type*

159 A linear modal testing analysis was used on the FE model to assess the vibration  
160 characteristics of the human femur. The modal analysis package of ANSYS software  
161 was used. To implement the numerical procedure, first the mode-extraction method to  
162 be used for the modal analysis is chosen. In this study, the Block Lanczos method is  
163 selected since it is a fast, efficient and robust algorithm to perform modal analysis.  
164 Next the frequency range has to be defined. To include the first five modes of  
165 vibrations, a range from 0 to 1000 Hz is taken.

166 A harmonic response analysis was also performed to obtain the vibration amplitude of  
167 the femur at a specific frequency range under a vertical load applied at the femoral  
168 head for the three different cases analyzed (condyle, diaphysis and physiological  
169 boundary conditions). This linear analysis has also been performed using the  
170 commercial software ANSYS. The harmonic response analysis method chosen is the  
171 Full method within a frequency range from 0 to 2000 Hz for all the boundary  
172 conditions analyzed.

173 The numerical analyses were run in a laptop PC Intel 1.8 GHz (1 core) with 8GB RAM.  
174 CPU time of the analyses was estimated in 8 minutes.

## 175 **3 Results**

176 Table 2 summarizes the dynamic characteristics of the femur analyzed. The first five  
177 natural frequencies as well as their corresponding modes of vibration are detailed for  
178 the different boundary conditions (BC) analyzed (free BC; diaphysis BC; condyle BC;  
179 physiological BC) and the two different material properties set-ups performed  
180 (constant mechanical properties and Hounsfield Units). The vibration plane of the

181 modes of vibration is specified: frontal bending, sagittal bending, combined bending  
182 (both frontal and sagittal bending) and torsion (T).

183 Natural frequencies range from 245 to 814 Hz for the free boundary conditions, 108 to  
184 887 Hz for the diaphysis boundary conditions, 222 to 803 Hz for the condyle boundary  
185 conditions and 107 to 782 Hz for the physiological boundary conditions. In order to  
186 compare qualitatively the four analyzed cases, the normalized natural frequencies for  
187 the different set-ups analyzed have been represented (fig. 2). Normalization has been  
188 performed with respect to the lowest frequency. It can be observed the moderate  
189 effect of material properties compared to the much substantial effect of boundary  
190 conditions. In particular, a high difference can be found from case to case of boundary  
191 conditions, being a factor higher than 2 in some frequencies. The biggest differences  
192 are found between free and condyle boundary conditions versus physiological ones.  
193 On the other hand, differences due to the fact of considering constant mechanical  
194 properties along the bone tissue are not so acute although important: a difference in  
195 the range 5-25% can be found for different boundary conditions across natural  
196 frequencies. Higher variations are found for the case of the condyle boundary  
197 conditions, whereas considering constant mechanical properties for the remaining  
198 cases is an assumable hypothesis (fig. 2).

199 To illustrate the modes of vibration for one of the set-ups analyzed, fig. 3 shows the  
200 deformed shape of the bone for the first five natural frequencies in the case of the  
201 physiological boundary conditions and constant mechanical properties assignment. It  
202 may be observed that sagittal bending modes are given at the first and fifth natural  
203 frequencies (fig. 3 and Table 2), frontal bending modes at the second and fourth  
204 natural frequencies and torsional mode at the third natural frequency. In the case of  
205 free boundary conditions, frontal bending modes are shown at the fourth natural  
206 frequency, sagittal bending modes at the fifth frequency, torsional mode at the third  
207 natural frequency and combined bending modes for the first and second natural  
208 frequencies (Table 2). For the diaphysis BC, frontal bending is shown for modes 1 and  
209 4, sagittal bending for modes 2 and 5 and torsional bending for mode 3. On the other  
210 hand, in the case of the condyle boundary conditions, Table 2 shows front sagittal  
211 modes at natural frequencies 1 and 4, frontal bending modes at 2 and 5 and torsional  
212 mode at the third natural frequency.

213 The results of the harmonic analysis are shown in fig. 4. It shows the dimensionless  
214 dynamic amplification factor, i.e. the vertical displacement vector, versus its  
215 corresponding value in a static analysis with the same loading conditions, in a spectral  
216 plot, for the different analyzed boundary conditions in the case in which material  
217 properties are assigned based on the HU method. As can be observed, the natural  
218 frequencies differed in the three cases as well as the amplitude of vibration pointing  
219 out the importance (quantitatively and qualitatively) of the boundary conditions  
220 chosen on the dynamical response obtained (fig. 4).

221

222

		Free BC		Diaphysis BC		Condyle BC		Physiological BC	
		Const	HU	Const	HU	Const	HU	Const	HU
1	$\omega_1$ (Hz)	271	245	111	108	276	222	146	107
	$\phi_1$	CB	CB	FB	FB	SB	SB	SB	SB
2	$\omega_2$ (Hz)	310	274	122	119	398	283	269	165
	$\phi_2$	CB	CB	SB	SB	FB	FB	FB	FB
3	$\omega_3$ (Hz)	660	567	592	531	468	378	330	240
	$\phi_3$	T	T	T	T	T	T	T	T
4	$\omega_4$ (Hz)	790	703	826	738	775	643	702	483
	$\phi_4$	FB	FB	FB	FB	SB	SB	FB	FB
5	$\omega_5$ (Hz)	814	760	887	861	803	716	782	619
	$\phi_5$	SB	SB	SB	SB	FB	FB	SB	SB

223

224

225

226

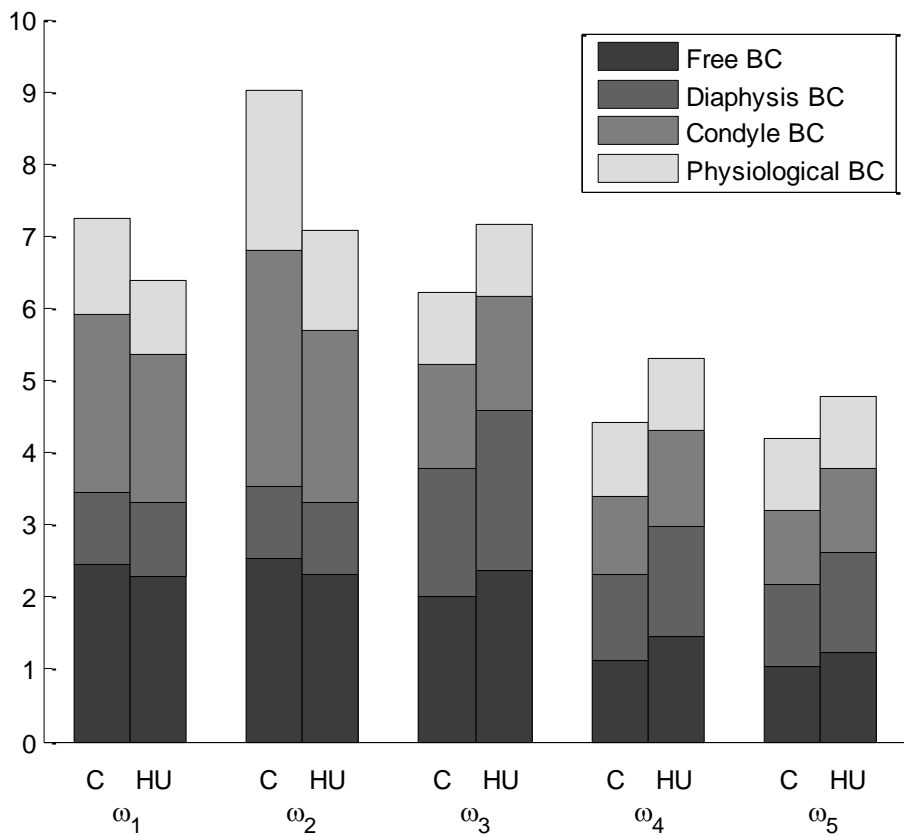
227

228

229

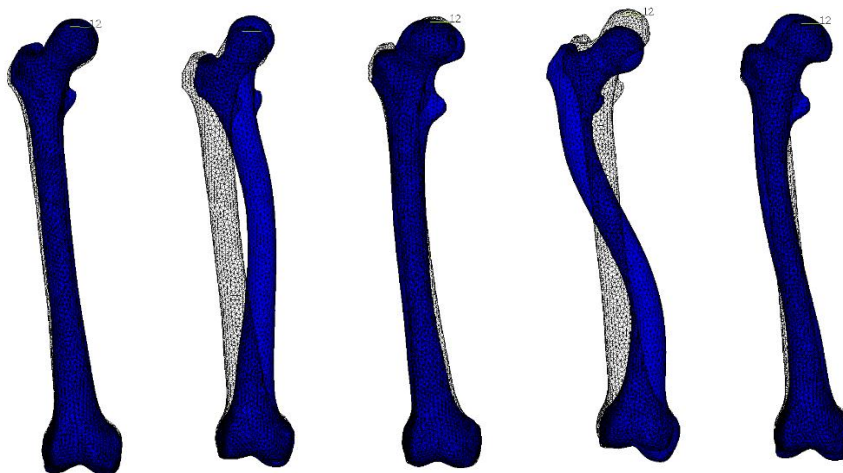
**Table 2.** Summary of the dynamic characteristics of the femur: natural frequencies  $\omega$  (Hz) and associated vibration modes  $\phi$ . Results are shown for the different analyzed boundary conditions (BC): free BC; diaphysis BC; condyle BC; physiological BC and for the two different material properties set-ups performed: constant mechanical properties (Const) and Hounsfield units (HU). For the modes of vibration, the corresponding vibration plane is specified: frontal bending (FB), sagittal bending (SB), combined bending (CB) and torsion (T).



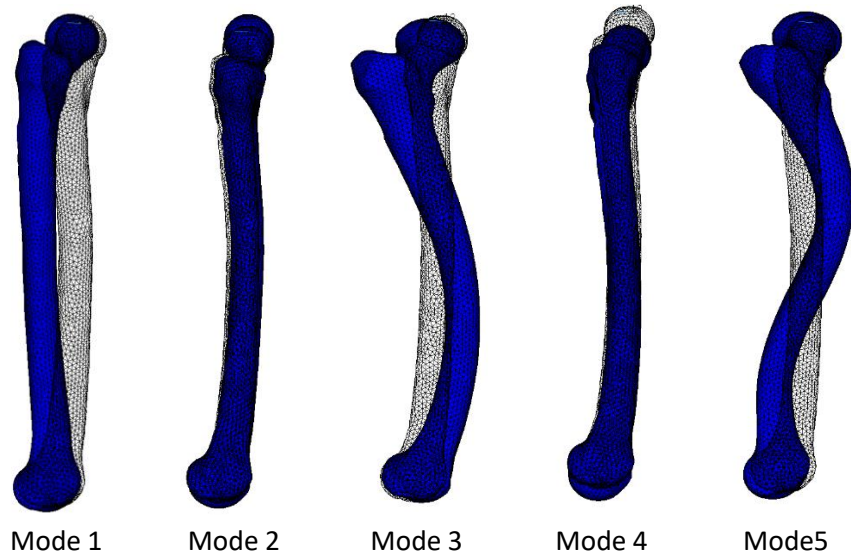


230  
231  
232  
233  
234  
235  
236

**Figure 2.** First 5 normalized natural frequencies ( $\omega$ ) of the femur under different analyzed boundary conditions (BC): free, diaphysis, condyle and physiological for the two mechanical properties assignment set-ups: constant mechanical properties (C) and Hounsfield Unit (HU). Normalization has been performed with respect to the lowest frequency for each set of analyzed boundary conditions and each natural frequency.

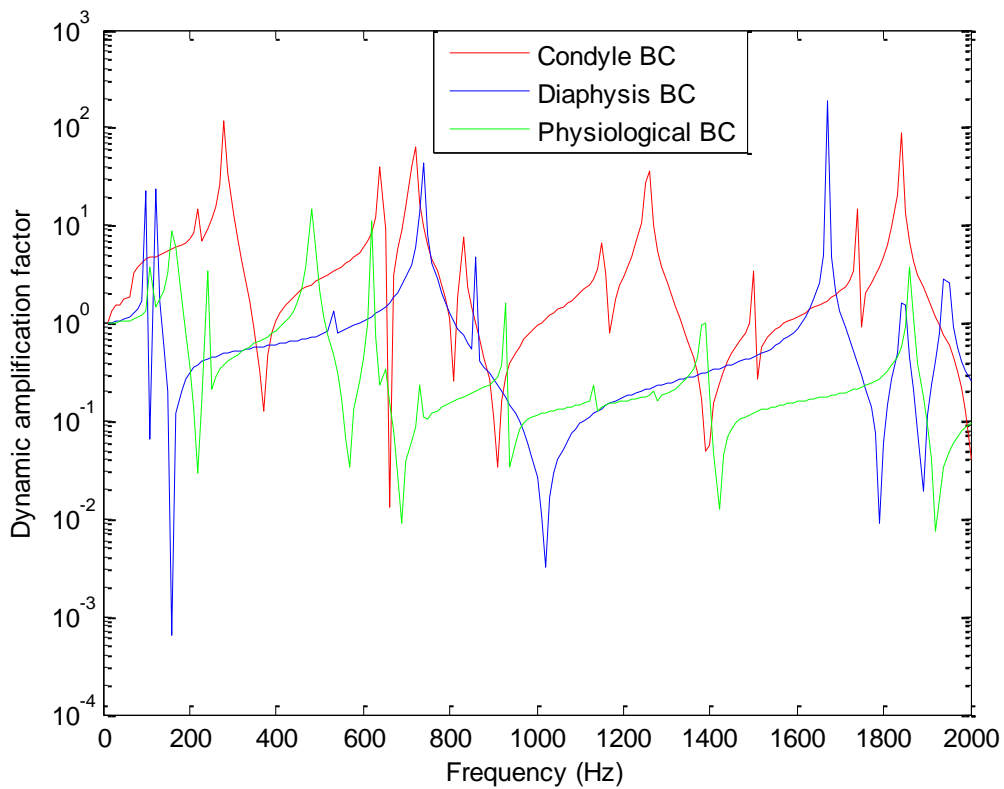


237



238

239 **Figure 3.** Vibration modes (associated to natural frequencies presented in table 2) of femur  
240 under physiological boundary conditions in the constant mechanical properties set-up. Upper  
241 part – frontal plane, bottom part – sagittal plane.



242

243

244

245

**Figure 4.** Dynamic amplification factor obtained for the condyle, diaphysis and physiological boundary conditions (BC) analyzed.

246 **4 Discussion**

247

248 The aim of the study presented in this paper was to highlight the great differences in  
249 the dynamic behavior (i.e. natural frequencies and vibration modes) of bone tissue  
250 when subjected to different boundary conditions. Differences are given not only  
251 referred as the value of natural frequency, but also on the shape of associated  
252 vibration modes as well as spectral dynamical behavior. As it can be seen in the results  
253 section, a proper selection of boundary conditions in modal analysis of femur is critical  
254 in order to establish right conclusions from such a study. On the one hand, free  
255 boundary conditions do not really represent actual boundary conditions of bone organ  
256 at physiological conditions. Nonetheless, they are commonly used as a benchmark and  
257 calibration of modal analysis of bone tissue, or even to establish analogies between  
258 bone tissue characteristics and (generic) dynamic behavior, both experimentally and  
259 numerically [14,20,22-23]. On the other hand, diaphysis boundary conditions at the  
260 bone organ are often used in different biomechanical analysis [19]. They are of  
261 application when some information of the geometry is missing, or even to alleviate  
262 computer resources of finite element analysis. However, as these conditions do not  
263 represent physiology of bone organ, they are not of application in a dynamic analysis  
264 nor can be of application as a model simplification hypothesis given the differences  
265 versus other implemented boundary conditions. Condyle boundary conditions are  
266 typically prescribed at surrounding locations where bone organ connect to other  
267 tissues, i.e. joints. They are used as well in a number of static biomechanical analyses  
268 and based on static equilibrium by prescribing displacements at these regions. Analysis  
269 and results are then of application far from the area where boundary conditions were  
270 applied. Again, condyle boundary conditions are non-physiological ones.

271

272 Conclusions taken of diaphysis and condyle boundary conditions for the dynamic case  
273 may not be of application at static conditions: in studies which consider static cases,  
274 boundary conditions are independently applied to find an equilibrated stress state,  
275 and hence equivalent, in the bone organ. Therefore, good fittings are found elsewhere  
276 in the literature when results are compared at these situations [31-32]. On the other  
277 hand, when the analysis is conducted in a dynamic scenario, results are strongly  
278 dependent on boundary conditions, as exposed in the present work, which have a  
279 minor importance in static problems.

280 The estimation of the dynamic characteristics of the human femur may contribute to  
281 improve the vibration therapies in bone tissue. For that purpose, physiological  
282 boundary conditions were selected as in Speirs et al. [27]. In that study authors  
283 conclude that such restrictions allow obtaining physiological levels of femur deflection  
284 when subjected to physiological range of forces. The analysis performed by the  
285 authors showed that other boundary conditions yielded to unreliable femur head  
286 deformations. Physiological boundary conditions are followed in other studies [33-34]

287 and are accepted as a reference for this kind of analysis. The biomechanical analysis  
288 presented in Speirs et al. [27] was static and its availability is extended here to the  
289 dynamic case. To the best of author's knowledge there is no reliable information about  
290 dynamic characteristics of human femur experimentally in order to compare and  
291 validate the analysis here presented.

292

293 There are several limitations of the study that should be commented. First, geometry  
294 has been taken from a single femur. Results of this study could be generalized using  
295 virtual models with different geometries [35]. Secondly, 10 different materials  
296 (mechanical properties) are chosen in this study in the HU set-up. According to Pérez &  
297 Seral-García [19], no significant resonance frequency changes occurred regardless of the  
298 number of material groups chosen. In addition, the effect of other bones and soft  
299 tissues of the musculoskeletal system and body on dynamic characteristics has been  
300 considered indirectly with the boundary conditions analyzed. Of course modeling them  
301 directly will dampen the vibration *in situ* and *in vivo*. However, this study is only the  
302 first step in understanding and dealing with the dynamic behavior of the femur.  
303 Additional experimental *in vivo* and *in vitro* studies are required to validate and  
304 improve the numerical modeling started with this study. These tasks are planned as a  
305 future work in the context of the present study.

306 The importance of predicting dynamic characteristic of bone tissues and organs has  
307 implications in many clinical scenarios. As it was reviewed in the introduction, vibration  
308 technique is a trending clinical therapy for bone mass regeneration under  
309 circumstances of bone disease such as osteoporosis [36]. There is not still a consensus  
310 on the protocol. However, whole body vibration is a promising technique [37-41] in  
311 which human body is subjected to cyclic vibration at different amplitudes in a range  
312 varying from 10-90 Hz [42]. In addition, frequencies in the range of resonance (natural  
313 frequency) of bone tissue provide positive outcomes as an alternative clinical therapy  
314 [43]. For this application, *a-priori* knowledge of bone tissue natural frequency is of  
315 critical importance in order to calibrate the setup of the clinical protocol. In a different  
316 context, knowledge of dynamic characteristics of bone tissues and organs has a great  
317 importance in the analysis of dynamic fracture behavior of bone [44] as well as long-  
318 term fatigue response of bone tissue to loads [45].

### 319 **Acknowledgements**

320 The authors gratefully acknowledge the research support of the Ministerio de  
321 Economía y Competitividad del Gobierno de España (DPI2014-58233-P, DPI2017-  
322 82501-P).

### 323 **Conflict of interest statement**

324 No conflict of interest to disclose.

325 **References**

- 326 [1] Nikander R, Kannus P, Dastidar P, Hannula M, Harrison L, Cervinka T, Narra  
327 NG, Aktour R, Arola T, Eskola H, Soimakallio S, Heinonen A, Hyttinen J, Sievänen H.  
328 Targeted exercises against hip fragility. *Osteoporos Int.* 2009; 20:1321-8.
- 329 [2] Hsieh YF, Turner CH. Effects of loading frequency on mechanically induced bone  
330 formation. *J Bone Miner Res* 2001; 16:918–924.
- 331 [3] Zhang P, Su M, Liu Y, Hsu A, Yokota H. Knee loading dynamically alters  
332 intramedullary pressure in mouse femora. *Bone* 2007; 40:538–543.
- 333 [4] Kameo Y, Adachi T, Hojo M. Effects of loading frequency on the functional  
334 adaptation of trabeculae predicted by bone remodeling simulation. *J Mech Behav*  
335 *Biomed Mater* 2011; 4:900–908.
- 336 [5] Tanaka SM, Alam IM, Turner CH. Stochastic resonance in osteogenic response to  
337 mechanical loading. *FASEB J* 2003; 17:313–314.
- 338 [6] Warden SJ, Turner CH. Mechanotransduction in the cortical bone is most efficient  
339 at loading frequencies of 5–10 Hz. *Bone* 2004; 34:261–270.
- 340 [7] Zhao L, Dodge T, Nemani A, Yokota H. Resonance in the mouse tibia as a predictor  
341 of frequencies and locations of loading-induced bone formation. *Biomech Model*  
342 *Mechanobiol* 2014; 13:141–151.
- 343 [8] Rubin C, Pope M, Fritton JC, Magnusson M, Hansson T, McLeod K. Transmissibility  
344 of 15-hertz to 35-hertz vibrations to the human hip and lumbar spine: determining the  
345 physiologic feasibility of delivering low-level anabolic mechanical stimuli to skeletal  
346 regions at greatest risk of fracture because of osteoporosis. *Spine* 2003; 28:2621–2627.
- 347 [9] Cardinale M, Rittweger J. Vibration exercise makes your muscles and bones  
348 stronger: fact or fiction?. *J Br Menopause Soc* 2006; 12:12-18.
- 349 [10] Zhang P, Su M, Tanaka SM, Yokota H. Knee loading stimulates cortical bone  
350 formation in murine femurs. *BMC Musculoskelet Disord* 2006; 7:73.
- 351 [11] Ozcivici E, Luu YK, Rubin CT, Judex S. Low-level vibrations retain bone marrow's  
352 osteogenic potential and augment recovery of trabecular bone during reambulation.  
353 *PLoS One* 2010; 5:e11178.
- 354 [12] Grimston SK, Watkins MP, Brodt MD, Silva MJ, Civitelli R. Enhanced periosteal and  
355 endocortical responses to axial tibial compression loading in conditional connexin43  
356 deficient mice. *PLoS One* 2012; 7:e44222.

- 357 [13] Silva MJ, Brodt MD, Hucker WJ. Finite element analysis of the mouse tibia:  
358 estimating endocortical strain during three-point bending in SAMP6 osteoporotic mice.  
359 *Anat Rec A Discov Mol Cell Evol Biol* 2005; 283:380–390.
- 360 [14] Couteau B, Hobatho MC, Darmana R, Brignola JC, Arlaud JY. Finite element  
361 modelling of the vibrational behaviour of the human femur using CT-based  
362 individualized geometrical and material properties. *J Biomech* 1998; 31:383-386.
- 363 [15] Nikiforidis G, Bezerianos A, Dimarogonas A, Sutherland C. Monitoring of fracture  
364 healing by lateral and axial vibration analysis. *J Biomech* 1990; 23:323–330.
- 365 [16] González-Torres LA, Gómez-Benito MJ, Doblaré M, García-Aznar JM. Influence of  
366 the frequency of the external mechanical stimulus on bone healing: a computational  
367 study. *Med Eng Phys* 2010; 32:363–371.
- 368 [17] Huang HM, Cheng KY, Chen CH, Lin CT, Lee SY. Design of a stability-detecting  
369 device for dental implants. *Proc Inst Mech Eng H* 2005; 219:203–211.
- 370 [18] Wang S, Liu GR, Hoang KC, Guo Y. Identifiable range of osseointegration of dental  
371 implants through resonance frequency analysis. *Med Eng Phys* 2010; 32:1094–1106.
- 372 [19] Pérez MA, Seral-García B. A finite element analysis of the vibration behaviour of a  
373 cementless hip system. *Comput Methods Biomech Biomed Engin* 2013; 16:1022-1031.
- 374 [20] Khalil TB, Viano DC, Taber LA. Vibrational characteristics of the embalmed human  
375 femur. *J Sound Vibr* 1981; 75:417-436.
- 376 [21] Glaser D, Komistek RD, Cates HE, Mahfouz MR. Clicking and squeaking: in vivo  
377 correlation of sound and separation for different bearing surfaces. *J Bone Joint Surg*  
378 *Am* 2008; 90:112–120.
- 379 [22] Campoli G, Baka N, Kaptein BL, Valstar ER, Zachow S. Relationship between the  
380 shape and density distribution of the femur and its natural frequencies of vibration. *J*  
381 *Biomech* 2014; 47:3334-3343.
- 382 [23] Pastrav LC, Devos J, van der Perre G, Jacques SVN. A finite element analysis of  
383 the vibrational behaviour of the intra-operatively manufactured prosthesis-femur  
384 system. *Med Eng Phys* 2009; 31:489-494.
- 385 [24] Weiss C, Gdaniec P, Hoffmann NP, Hothan A, Huber G, Morlock MM. Squeak in hip  
386 endoprosthesis systems: an experimental study and a numerical technique to analyze  
387 design variants. *Med Eng Phys* 2010; 32:604–609.
- 388 [25] Knothe Tate ML, Steck R, Anderson EJ. Bone as an inspiration for a novel class of  
389 mechanoactive materials. *Biomaterials* 2009; 30: 133-40.

- 390 [26] Knothe Tate ML. Top down and bottom up engineering of bone. *J Biomech* 2011;  
391 44: 304-12.
- 392 [27] Speirs AD, Heller MO, Duda GN, Taylor WR. Physiologically based boundary  
393 conditions in finite element modeling. *J Biomech* 2007; 40:2318–2323.
- 394 [28] Ward DA, Robinson KP. Osseointegration for the skeletal fixation of limb  
395 prostheses in amputations at the trans-femoral level, in: *The Osseointegration Book*  
396 *from Calvarium to Calcaneus*, edited by P-I. Branemark, S. Chien, H-G Grondahl, and K.  
397 Robinson. Berlin: Quintessenz Verlags-GmbH, 2005 pp. 463-476.
- 398 [29] Beaupre GS, Orr TE, Carter DR. An approach for time-dependent bone modeling  
399 and remodeling-theoretical development. *J Orthop Res* 1990; 8:651-661.
- 400 [30] Cutnell JD, Johnson KW, Young D, Stadler S. *Physics*, 10th Edition. Wiley, 2015.
- 401 [31] Doblaré M, García JM. Application of an anisotropic bone-remodelling model  
402 based on a damage-repair theory to the analysis of the proximal femur before and  
403 after total hip replacement. *J Biomech* 2001; 34:1157–1170.
- 404 [32] Sanz-Herrera JA, García-Aznar JM, Doblaré M. Micro–macro numerical modelling  
405 of bone regeneration in tissue engineering. *Comput Meth Appl Mech Eng* 2008;  
406 197:3092-3107.
- 407 [33] Bayoglu R, Okyar AF. Implementation of boundary conditions in modeling the  
408 femur is critical for the evaluation of distal intramedullary nailing. *Med Eng Phys* 2015;  
409 37:1053-1060.
- 410 [34] Grassi L, Schileo E, Boichon C, Viceconti M, Taddei F. Comprehensive evaluation of  
411 PCA-based finite element modelling of the human femur. *Med Eng Phys* 2014;  
412 36:1246-1252.
- 413 [35] Moore SR, Milz S, Knothe Tate ML. The linea aspera: a virtual case study testing  
414 emergence of form and function. *Anat Rec (Hoboken)*. 2014; 297: 273-80.
- 415 [36] Beck RB. Vibration Therapy to Prevent Bone Loss and Falls: Mechanisms and  
416 Efficacy. *Curr Osteoporos Rep* 2015; 13: 381–389.
- 417 [37] Pel JJ, Bagheri J, van Dam LM, van den Berg-Emons HJ, Horemans HL, Stam HJ, van  
418 der Steen J. Platform accelerations of three different wholebody vibration devices and  
419 the transmission of vertical vibrations to the lower limbs. *Med Eng Phys* 2009; 31:937–  
420 944.
- 421 [38] Rubin C, Turner AS, Bain S, Mallinckrodt C, McLeod K. Low mechanical signals  
422 strengthen long bone. *Nature* 2001; 412.

- 423 [39] Kiiski J, Heinonen A, Jarvinen TL, Kannus P, Sievanen H. Transmission of vertical  
424 whole body vibration to the human body. *J Bone Miner Res* 2008; 23:1318–1325.
- 425 [40] Matsumoto Y, Griffin M. Dynamic response of the standing human body exposed  
426 to vertical vibration: influence of posture and vibration magnitude. *J Sound Vibr* 1998;  
427 212:85–107.
- 428 [41] Crewther B, Cronin J, Keogh J. Gravitational forces and whole body vibration:  
429 implications for prescription of vibratory stimulation. *Phys Ther Sport* 2004; 5:37–43.
- 430 [42] Pasqualini M, Lavet C, Elbadaoui M, Vanden-Bossche A, Laroche N, Gnyubkin V,  
431 Vico L. Skeletal site-specific effects of whole body vibration in mature rats: from  
432 deleterious to beneficial frequency dependent effects. *Bone* 2013; 55:69–77.
- 433 [43] Dionello CF, Sá-Caputo D, Pereira HV, Sousa-Gonçalves CR, Maiworm AI, Morel DS,  
434 Moreira-Marconi E, Paineiras-Domingos LL, Bembem D, Bernardo-Filho M. Effects of  
435 whole body vibration exercises on bone mineral density of women with  
436 postmenopausal osteoporosis without medications: Novel findings and literature  
437 review. *J Musculoskelet Neuronal Interac* 2016; 16:193-203.
- 438 [44] Nyman JS, Granke M, Singleton RC, Pharr GM. Tissue-Level Mechanical Properties  
439 of bone contributing to fracture risk. *Curr Osteoporos Rep* 2016; 14:138-150.
- 440 [45] Matcuk GR, Mahanty SR, Skalski MR, Patel DB, White EA, Gottsegen CJ. Stress  
441 fractures: Pathophysiology, clinical presentation, imaging features, and treatment  
442 options. *Emerg Radiol* 2016; 23:365-375.
- 443